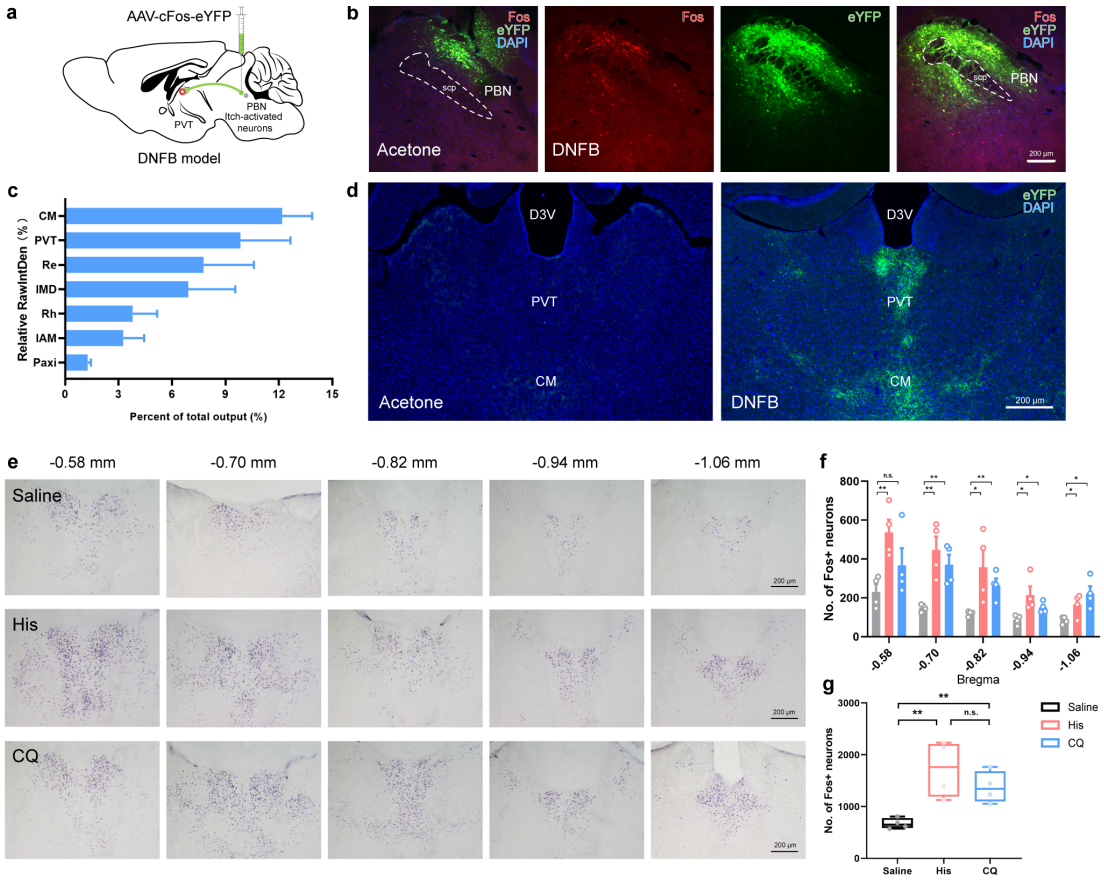

Figure S1. The participation of the PVT in itch modulation process.

a, Schematic diagram of virus injection into the PBN performed with DNFB model.

b, Injection sites depicting the location of itch-activated AAV virus (green) and Fos-immunoreactive (red) neurons with DAPI delineating the PBN. Scale bar: 200 μm.

c, Percentages of the eGFP-labeled fibers and terminals from the midline nuclei in the total output in the thalamus (n=3).

d, The distribution pattern of the eGFP-labeled terminals in Acetone and DNFB groups. Scale bar: 200 μm.

e, The Fos distribution pattern in PVT from mice applied with Saline, His or CQ. Scale bars: 200 μm.

f, Summary data of the Fos^+ neurons in representative bregma of PVT. Two-tailed unpaired Student's t-test: bregma = -0.58 mm, $P = 0.007$ for Saline vs. His, $P = 0.2055$ for Saline vs. CQ; bregma = -0.70 mm, $P = 0.0052$ for Saline vs. His, $P = 0.0054$ for Saline vs. CQ; bregma = -0.82 mm, $P = 0.0369$ for Saline vs. His, $P = 0.0064$ for Saline vs. CQ; bregma = -0.94 mm, $P = 0.0348$ for Saline vs. His, $P = 0.0154$ for Saline vs. CQ; bregma = -1.06 mm, $P = 0.0361$ for Saline vs. His, $P = 0.012$ for Saline vs. CQ.

g, Summary data of Fos^+ neurons in mice applied with Saline (n=4), His (n=4) or CQ (n=4). Two-tailed unpaired Student's t-test: $P = 0.0093$ for Saline vs. His, $P = 0.0047$ for Saline vs. CQ, $P = 0.3124$ for His vs. CQ.

Data are presented as the boxplot or mean ± SEM. n.s.: no significance, *$P < 0.05$, **$P < 0.01$. CM: Central medial thalamic nucleus. Re: Reuniens thalamic nucleus, IMD: Intermediodorsal thalamic nucleus, Rh: rhomboid thalamic nucleus, IAM: Interanteromedial thalamic nucleus, Paxi: paraxiphoid nucleus of thalamus, scp: Superior cerebellar pedduncle, D3V: Dorsal 3rd ventricle, DNFB: 1-fluoro-2,4-dinitrobenzene.

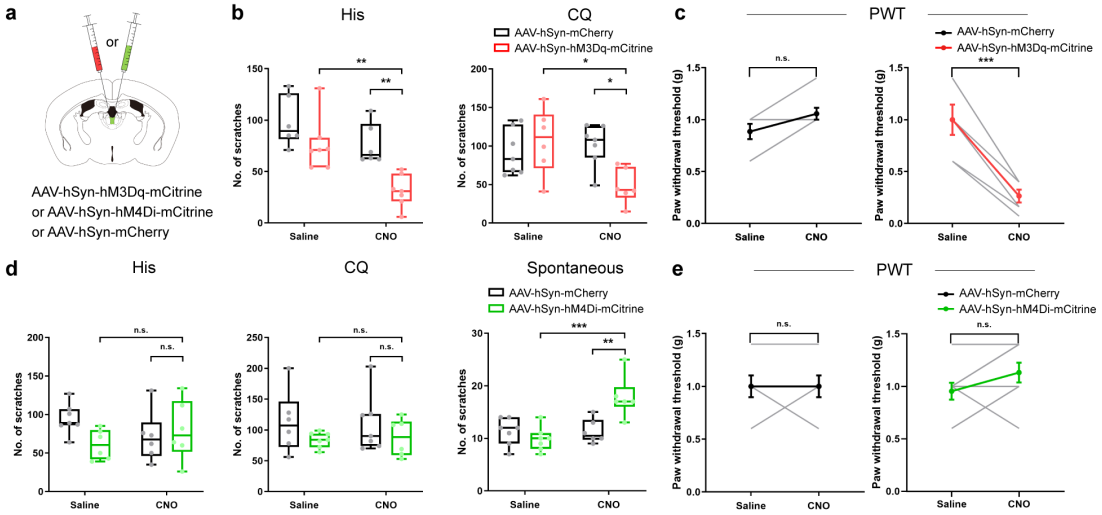

Figure S2. Chemogenic PVT activation attenuated scratching behavior yet induced allodynia.

a, Schematic diagram of the PVT chemogenic activation or inhibition.

b, PVT activation significantly suppressed the number of scratches in both His- and CQ-induced acute itch models (n = 6-7). Left: His-induced itch, interaction effect $F_{(1,22)}$ = 1.752, P = 0.1992, P = 0.0042 for hM3Dq-expressing mice with Saline vs. CNO, P = 0.0064 for CNO-treated mice with mCherry vs. hM3Dq. Right: CQ-induced itch, interaction effect $F_{(1,22)}$ = 7.629, P = 0.0114, P = 0.0179 for hM3Dq-expressing mice with Saline vs. CNO, P = 0.0272 for CNO-treated mice with mCherry vs. hM3Dq.

c, Paw withdrawal threshold decreased after chemogenic PVT activation in naive mice (n = 6-7). Left: P = 0.0781 for mCherry control mice with Saline vs. CNO; Right: P = 0.0007 for hM3Dq-expressing mice with Saline vs. CNO.

d, Summary data of PVT chemogenic inhibition in acute and spontaneous itch (n=6-7). Left: His-induced itch, interaction effect $F_{(1,21)}$ = 3.339, P = 0.0819, P = 0.6758 for hM4Di-expressing mice with Saline vs. CNO, P = 0.9547 for CNO-treated mice with mCherry vs. hM4Di. Middle: CQ-induced itch, interaction effect $F_{(1,22)}$ = 0.04771, P = 0.8291, P = 0.998 for hM4Di-expressing mice with Saline vs. CNO, P = 0.7176 for CNO-treated mice with mCherry vs. hM4Di. Right: Spontaneous itch, interaction effect $F_{(1,22)}$ = 12.95, P = 0.0016, P = 0.0002 for hM4Di-expressing mice with Saline vs. CNO, P = 0.0030 for CNO-treated mice with mCherry vs. hM4Di.

e, Summary data of PVT chemogenic inhibition in PWT (n=6-9). Left: P > 0.9999 for mCherry control mice with Saline vs. CNO. Right: P = 0.1038 for hM4Di-expressing mice with Saline vs. CNO.

Data are presented as the boxplot or mean ± SEM. n.s.: no significance, *P < 0.05, ** P< 0.01, ***P < 0.001. Two-way ANOVA with Tukey's multiple comparison tests for **b** and **d**, and two-tailed, paired,

Student's t-test for **c** and **e**.

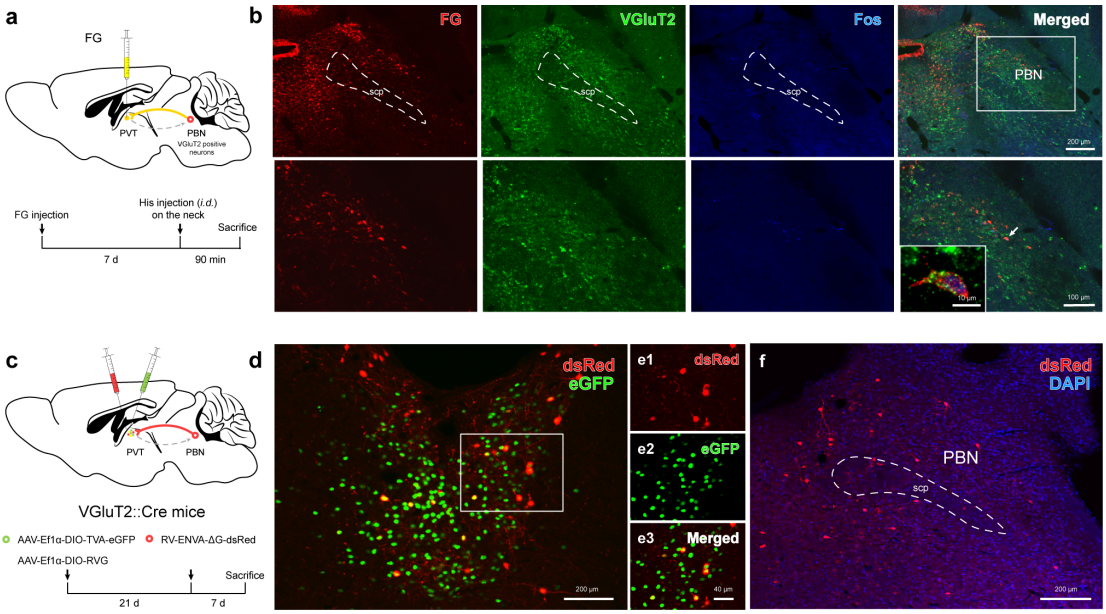

Figure S3. The glutamatergic nature of the PBN-PVT projection.

a, Schematic diagram and time line of the FG injection into the PVT.

b, Representative images of Fos immunoreactivity (blue) in VGluT2 mRNA positive (green) and FG-labeled neurons (red). White square is enlarged and VGluT2 mRNA-/Fos-/FG-triple-labeled neurons pointed with white arrow is displayed as insert image. Scale bars: 200 μm (upper), 100 μm (lower) and 10 μm (insert).

c, Schematic diagram of RV-virus injection into the PVT of VGluT2::Cre mouse.

d-e, Representative images of PVT neurons expressing RV virus. White square is enlarged and neurons co-expressed with rabies-dsRed (red) and eGFP (green) were identified as starter cells. Scale bars: 200 μm (**d**) and 40 μm (**e**).

f, Representative image showing retrograde labeling in the PBN. Scale bar: 200 μm.

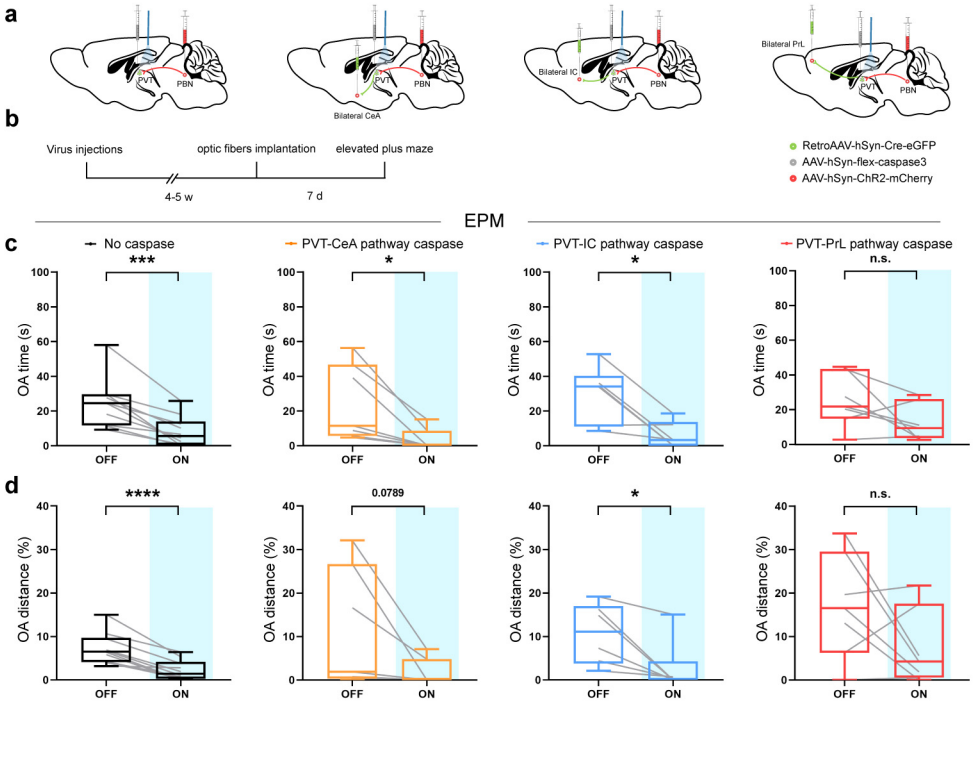

Figure S4. Distinct modulatory effects of different PBN-PVT downstream pathways in EPM.

a-b, The schematic diagram and time line indicating the virus strategy for PBN-PVT pathway-specific excitation with caspase-induced PVT^{CeA}, PVT^{IC} or PVT^{PrL} apoptosis.

c, Statistics of the time spent in open arm (OA time) after the PBN-PVT pathway activation with or without PVT^{CeA}, PVT^{IC} or PVT^{PrL} neurons. No caspase: n=10, light-off vs. light-on, P = 0.0003; PVT^{CeA} caspase: n=7, light-off vs. light-on, P = 0.0192; PVT^{IC} caspase: n=6, light-off vs. light-on, P = 0.0173; PVT^{PrL} caspase: n=7, light-off vs. light-on, P = 0.0989.

d, The modulatory effects of the PBN-PVT pathway activation with or without PVT^{CeA}, PVT^{IC} or PVT^{PrL} in the percentages of distance traveled in open arm (OA distance). No caspase: n=10, light-off vs. light-on, $P < 0.0001$; PVT^{CeA} caspase: n=7, light-off vs. light-on, P = 0.0789; PVT^{IC} caspase: n=6, light-off vs. light-on, P = 0.0251; PVT^{PrL} caspase: n=7, light-off vs. light-on, P = 0.1355.

Data are presented as boxplot. n.s.: no significance, $*P < 0.05$, $***P < 0.001$, $****P < 0.0001$. Two-tailed, paired, Student's t-test for **c** and **d**.

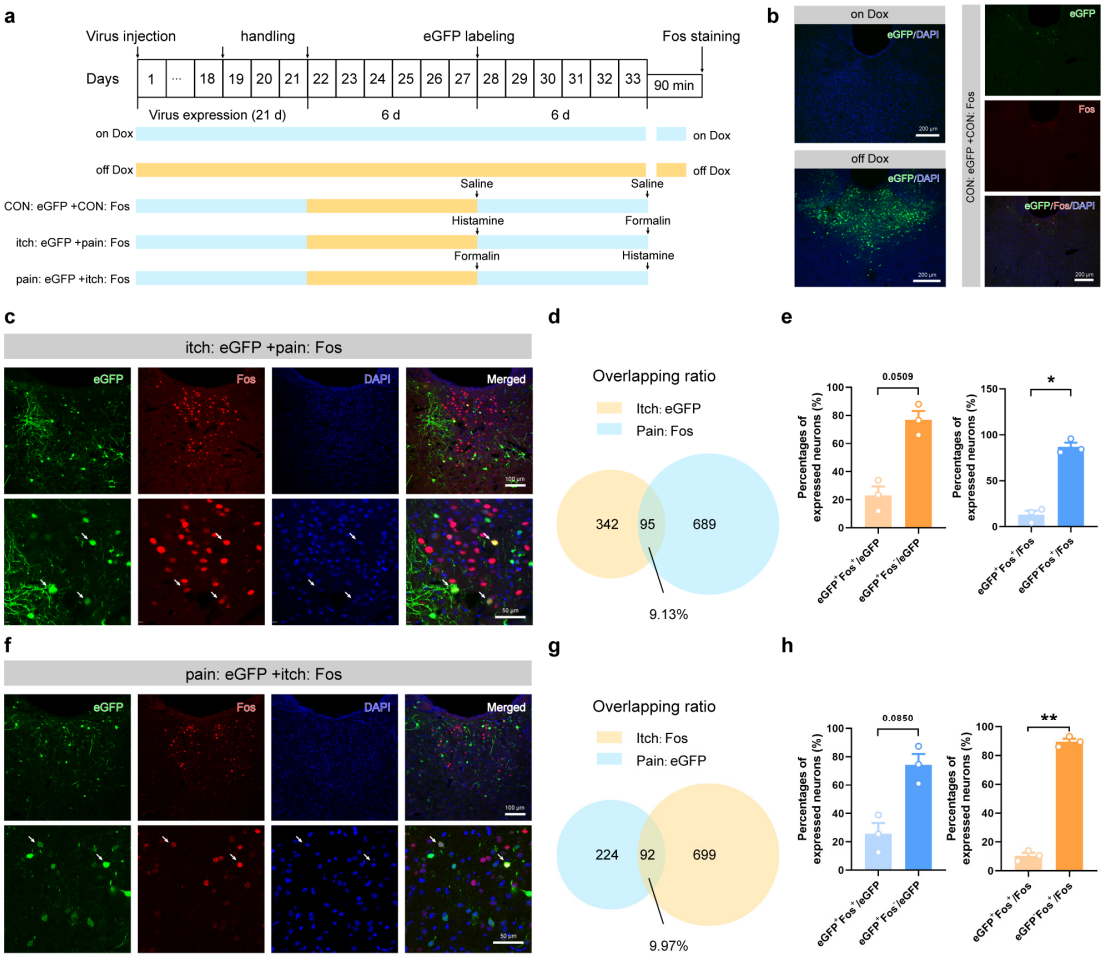

Figure S5. The itch- and pain-activated neurons in the PVT with little overlapping.

a, The virus strategy, time line and experimental design for labeling itch- and pain-activated neurons in the PVT.

b, Representative images of eGFP expression with or without doxycycline (Dox) and in CON: eGFP + CON: Fos group. Scale bars: 200 μm.

c, Representative images of endogenous Fos activated by pain (red) that co-labeled with $eGFP^+$ itch-activated neurons (green) in the PVT. Scale bars: 100 μm (upper) and 50 μm (lower).

d, Overlapping ratio of pain-activated (Fos^+) and itch-activated ($eGFP^+$) neurons in the PVT.

e, Percentages of double-labeled neurons among $eGFP^+$ and Fos^+ neurons were lower than that of single-labeled neurons. Left: $eGFP^+Fos^+$/eGFP vs. $eGFP^+Fos^-$/eGFP, P = 0.0509. Right: $eGFP^+Fos^+$/Fos vs. $eGFP^-Fos^+$/Fos, P = 0.0141.

f, Representative images of endogenous Fos activated by itch (red) that co-labeled with $eGFP^+$ pain-activated neurons (green) in the PVT. Scale bars: 100 μm (upper) and 50 μm (lower).

g, Overlapping ratio of pain-activated ($eGFP^+$) and itch-activated (Fos^+) neurons in the PVT.

h, Percentages of double-labeled neurons among $eGFP^+$ and Fos^+ neurons were lower than that of single-labeled neurons. Left: $eGFP^+Fos^+$/eGFP vs. $eGFP^+Fos^-$/eGFP, $P = 0.0850$. Right: $eGFP^+Fos^+$/Fos vs. $eGFP^-Fos^+$/Fos, $P = 0.0027$.

Data are presented as mean ± S.E.M. *$P < 0.05$, **$P < 0.01$. Two-tailed, paired, Student's t-test for **e** and **h**. CON: control group.

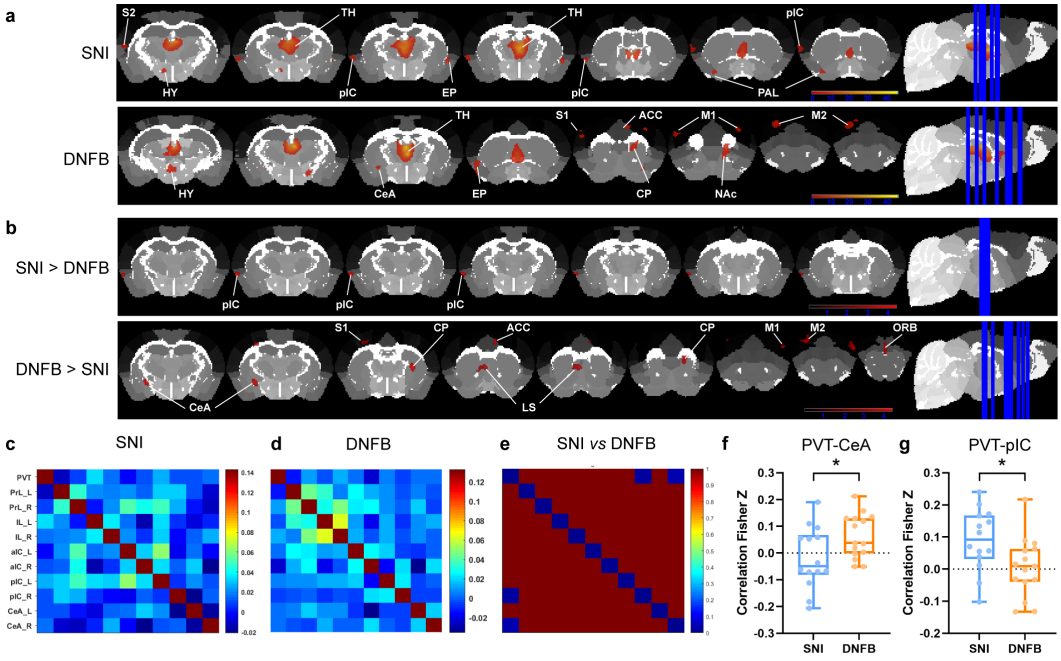

Figure S6. Differences in functional connectivity between the SNI and DNFB models.

a-b, Voxel-wise FC analysis with the PVT seed in the SNI and DNFB groups and corresponding difference maps between the groups (SNI, n=14; DNFB, n=15). Red/orange represents anatomical location of voxels with increased FC. The color bars represent *T* values. One-tailed unpaired Student's t-test for **a** and Two-tailed unpaired Student's t-test for **b**, uncorrected $P < 0.005$, minimal cluster size 50 voxels.

c-e, ROI-wise FC analysis among the PVT, bilateral PrL, IL, aIC, pIC and CeA. **c-d**, Mean correlation coefficients in the SNI (**c**) and DNFB (**d**) groups. **e**, Comparisons between the groups revealed different FC between the PVT with pIC and CeA. Two-tailed unpaired Student's t-test for E, uncorrected $P < 0.05$.

f-g, Regional quantification of the mean FC Z values revealed the significantly different FC between SNI and DNFB groups. Two-tailed unpaired Student's t-test for **f** and **g**, uncorrected $P < 0.05$.

Data are presented as boxplot. *$P < 0.05$. M1: Primary motor area, M2: Secondary motor area, S1: Primary somatosensory area, S2: Supplemental somatosensory area, aIC: Insular area, anterior part, pIC: Insular area, posterior part, ACC: Anterior cingulate cortex, ORB: Orbital area, EP: Endopiriform nucleus, PAL: Pallidum, CP: Caudoputamen, NAc: Nucleus accumbens, LS: Lateral septal nucleus, CeA:

Central amygdala nucleus, HY: Hypothalamus, TH: Thalamus.

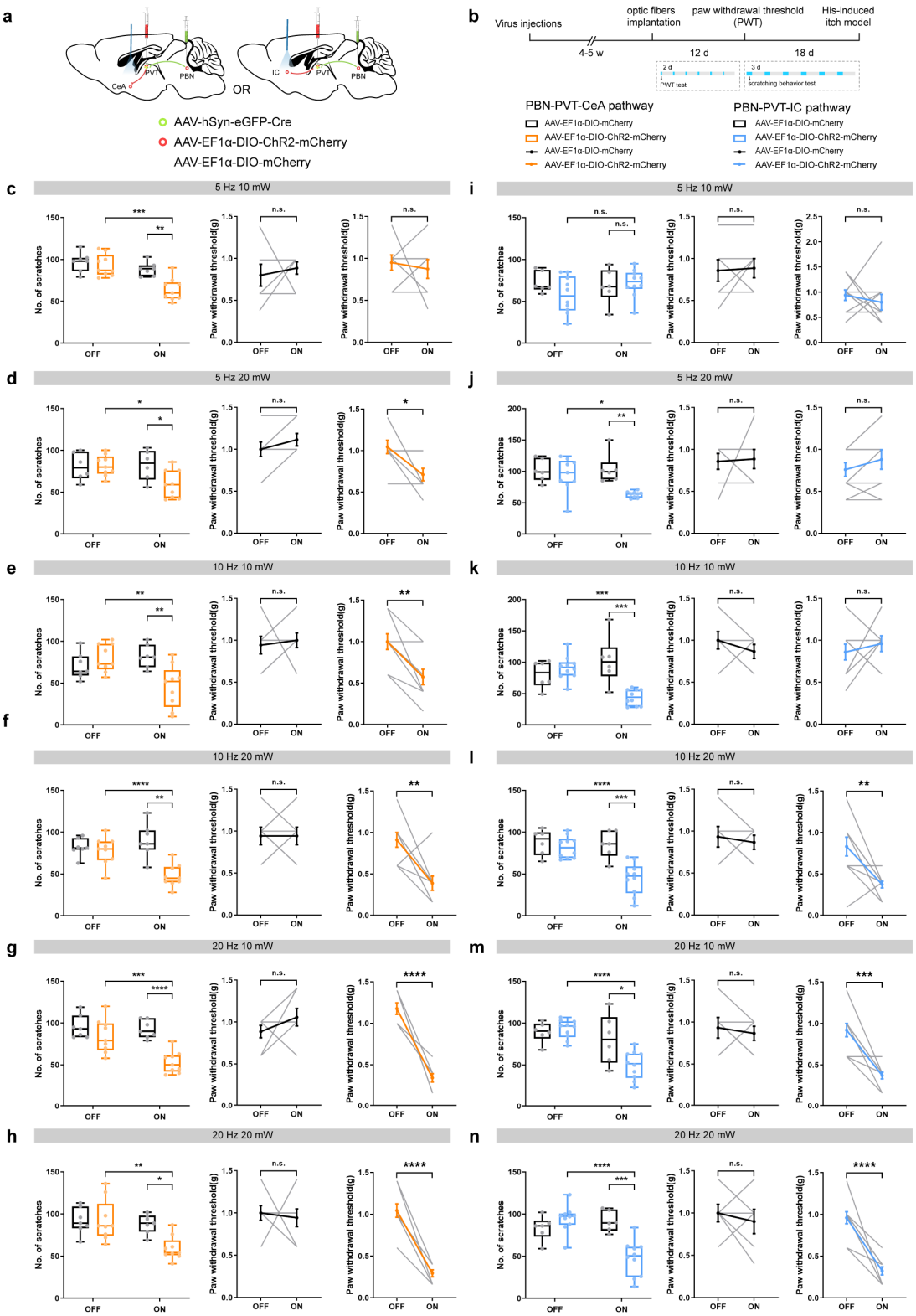

Figure S7. The modulatory effects of the PBN-PVT-CeA/IC pathways are intensity-dependent.

a-b, Schematic diagram of virus injection and optic fibers implantation to activate the PBN-PVT-CeA and PBN-PVT-IC pathway, respectively.

c-h, Statistics of the No. of scratches (left) and PWT (middle and right) with the PBN-PVT-CeA pathway light stimulation under various stimulation patterns. **c**, Light stimulated with 5Hz, 10mW, (left) No. of scratches, n = 7-9, $F_{(1,28)}$= 5.858, P = 0.0222, P = 0.0001 for ChR2-expressing mice with light-off vs. light-on, P = 0.0019 for mCherry vs. ChR2 during light-on. PWT, (middle) n = 7, P = 0.6394 for mCherry control mice with light-off vs. light-on, (right) n = 8, P = 0.6537 for ChR2-expressing mice with light-off vs. light-on. **d**, 5Hz, 20mW, (left) n = 6-9, $F_{(1,26)}$= 4.162, P = 0.0516, P = 0.0281 for light-off vs. light-on, P = 0.0477 for mCherry vs. ChR2 during light-on; (middle) n = 7, P = 0.1723 for light-off vs. light-on; (right) n = 9, P = 0.0203 for light-off vs. light-on. **e**, 10Hz, 10mW, (left) n = 7-8, $F_{(1,28)}$= 11.54, P = 0.0021, P = 0.0033 for light-off vs. light-on, P = 0.0038 for mCherry vs. ChR2 during light-on; (middle) n = 7, P = 0.7358 for light-off vs. light-on; (right) n = 9, P = 0.0016 for light-off vs. light-on. **f**, 10Hz, 20mW, (left) n = 7-9, $F_{(1,28)}$= 11.86, P = 0.0018, P = 0.0018 for light-off vs. light-on, P < 0.0001 for mCherry vs. ChR2 during light-on; (middle) n = 7, P > 0.9999 for light-off vs. light-on; (right) n = 9, P = 0.0056 for light-off vs. light-on. **g**, 20Hz, 10mW, (left) n = 7-9, $F_{(1,28)}$= 7.000, P = 0.0132, P = 0.0008 for light-off vs. light-on, P < 0.0001 for mCherry vs. ChR2 during light-on; (middle) n = 7, P = 0.2894 for light-off vs. light-on; (right) n = 9, P < 0.0001 for light-off vs. light-on. **h**, 20Hz, 20mW, (left) n = 7-9, $F_{(1,28)}$= 5.540, P = 0.0258, P = 0.0023 for light-off vs. light-on, P = 0.0133 for mCherry vs. ChR2 during light-on; (middle) n = 7, P = 0.7663 for light-off vs. light-on; (right) n = 9, P < 0.0001 for light-off vs. light-on.

i-n, Statistics of the No. of scratches (left) and PWT (middle and right) with the PBN-PVT-IC pathway light stimulation under various stimulation patterns. **i**, Light stimulated with 5Hz, 10mW, (left) No. of scratches, n = 6-10, $F_{(1,28)}$= 1.922, P = 0.1765, P = 0.3301 for ChR2-expressing mice with light-off vs. light-on, P = 0.9823 for mCherry vs. ChR2 during light-on. PWT, (middle) n = 7, P = 0.8461 for mCherry control mice with light-off vs. light-on, (right) n = 10, P = 0.5152 for ChR2-expressing mice with light-off vs. light-on. **j**, 5Hz, 20mW, (left) n = 6-9, $F_{(1,26)}$= 4.988, P = 0.0343, P = 0.0145 for light-off vs. light-on, P = 0.0039 for mCherry vs. ChR2 during light-on; (middle) n = 7, P = 0.877 for light-off vs. light-on; (right) n = 10, P = 0.1114 for light-off vs. light-on. **k**, 10Hz, 10mW, (left) n = 6-10, $F_{(1,28)}$= 17.47, P = 0.0003, P = 0.0004 for light-off vs. light-on, P = 0.0001 for mCherry vs. ChR2 during light-on; (middle) n = 6, P = 0.3632 for light-off vs. light-on; (right) n = 10, P = 0.5505 for light-off vs. light-on. **l**, 10Hz, 20mW, (left) n = 6-10, $F_{(1,28)}$= 8.737, P = 0.0063, P < 0.0001 for light-off vs. light-on, P < 0.0002 for mCherry vs. ChR2 during light-on; (middle) n = 6, P = 0.6952 for light-off vs. light-on; (right) n = 10, P

= 0.0048 for light-off vs. light-on. **m**, 20Hz, 10mW, (left) n =6-10, $F_{(1,28)}$= 6.962, P = 0.0134, P < 0.0001 for light-off vs. light-on, P = 0.0116 for mCherry vs. ChR2 during light-on; (middle) n = 6, P = 0.6952 for light-off vs. light-on; (right) n = 10, P = 0.0002 for light-off vs. light-on. **n**, 20Hz, 20mW, (left) n = 7-9, $F_{(1,28)}$= 19.74, P = 0.0001, P < 0.0001 for light-off vs. light-on, P = 0.0002 for mCherry vs. ChR2 during light-on; (middle) n = 6, P = 0.5965 for light-off vs. light-on; (right) n = 10, P < 0.0001 for light-off vs. light-on.

Data are presented as the boxplot or mean ± SEM. n.s.: no significance, *P < 0.05, **P < 0.01, ***P < 0.001, ****P < 0.0001. Two-tailed, paired, Student's t-test for PWT test in **c-n**, and two-way ANOVA with Tukey's multiple comparison tests for No. of scratches in **c-n**.

Supplementary table 1. Viruses and drugs utilized for morphological and behavioral experiments

	Experimental purposes	Viruses/Drugs	Location/ Target nuclei	Volume	Serotype	Serial Number
Morphological	Fos expression	His/CQ/Saline	nape	15 μl		
experiments		Formalin	planter	15 μl		
		Acetone/DNFB	nape			
		AAV-cFos-tTA-NLS-FLAG	PVT	100 nl	AAV2/9	BC221118-0058-9
		AAV-TRE-tight-eGFP	PVT	100 nl	AAV2/9	BC230804-2296-9
	Retrograde	4% Fluoro-gold (FG)	PVT	20 nl		
	tracing	4% Fluoro-gold (FG)	right CeA, IC, PrL	20 nl		
		594-Retrobeads	right CeA	150 nl		
		CTB	right IC	150 nl		
		488-Retrobeads	CeA, IC, PrL	150 nl		
		AAV-Ef1α-DIO-TVA-eGFP	PVT	150 nl	AAV2/9	PT-0021
		AAV-Ef1α-DIO-RVG	PVT	150 nl	AAV2/8	PT-0023
		RV-ENVA-ΔG-dsRed	PVT	150 nl		R01002
	Anterograde	AAV-cFos-eYFP	right PBN	150 nl	AAV2/9	PT-0129
	tracing	AAV-CMV bGlobin-Cre-mCherry	PBN	150 nl	AAV2/1	S0702-1
		AAV-hSyn-DIO-eGFP	PVT	150 nl	AAV2/9	PT-1103
Behavioral	Baseline	His/CQ/Saline	nape	15 μl		
experiments		Acetone/DNFB	nape			
	Fiber photometry	AAV-hSyn-GCaMP7s	PVT	150 nl	AAV2/9	PT-1890
	Pharmacological	AAV-CMV bGlobin-Cre-eGFP	PVT	150 nl	AAV2/2 Retro	S0231-2
	manipulation	AAV-hSyn-DIO-hM3Dq-mCherry	Bilateral PBN	150 nl	AAV2/9	PT-0019
		AAV-hSyn-DIO-hM4Di-mCherry	Bilateral PBN	150 nl	AAV2/9	PT-0020
		AAV-hSyn-DIO-mCherry	Bilateral PBN	150 nl	AAV2/9	PT-0115
		AAV-hSyn-hM3Dq-mCitrine	PVT	100 nl	AAV2/9	H3451
		AAV-hSyn-hM4Di-mCitrine	PVT	100 nl	AAV2/9	H3452
		AAV-hSyn-mCherry	PVT	100 nl	AAV2/9	PT-0100
	Optogenetic	AAV-hSyn-EGFP-P2A-Cre	right PBN	150 nl	AAV2/1	BC-0160
	manipulation	AAV-EF1α-DIO-hChR2(H134R)-mCherry	PVT	150 nl	AAV2/9	BC-0108
		AAV-EF1α-DIO-mCherry	PVT	150 nl	AAV2/9	PT-0013
		AAV-CaMKII-mCherry	PBN	150 nl	AAV2/9	PT-0108
		AAV-CMKII-ChR2-mCherry	PBN	150 nl	AAV2/9	PT-0297
	Apoptosis	AAV-hSyn-flex-caspase3	PVT	150 nl	AAV2/9	PT-0206
	manipulation	AAV-hSyn-Cre-eGFP	Bilateral CeA, IC, PrL	150 nl	AAV2/R	PT-1399
		AAV-hSyn-ChR2-mCherry	PBN	150 nl	AAV2/9	PT-0150

*: AAV-CMVbGlobin-Cre-mCherry were provided by Shanghai Taitool Bioscience Co. Ltd. Other viruses were provided by Wuhan Brain VTA Co. Ltd.

Supplementary table 2. Antisera used for FISH staining and immunofluorescent staining

Groups	Primary antisera	Secondary antisera	Tertiary antisera
594-Retrobeads/CTB/FG	Goat anti-CTB (1:500, 703, Iistlabs) Rabbit anti-FG antibody (1:500, AB153-I, Merck Millipore)	Alexa 488 donkey anti-goat (1:500, a11055, Invitrogen) Alexa 647 donkey anti- rabbit (1:500, A31573, Invitrogen)	
eGFP/Fos/FG	Mouse anti-Fos (1:500, ab11959, Abcam) Rabbit anti-FG antibody (1:500, AB153-I, Merck Millipore)	Alexa 647 donkey anti- mouse (1:500, A31571, Invitrogen) Alexa 594 donkey anti-rabbit (1:500, A21207, Invitrogen)	
Fos/eYFP/DAPI	Mouse anti-Fos (1:500, ab11959, Abcam)	Alexa 594 donkey anti-mouse (1:500, A21203, Invitrogen)	DAPI (1:500, sc-3598, Santacruz, TX, USA)
FG/VGluT2 /Fos	VGluT2 riboprobes	Anti-digoxigenin sheep antibody (1:1500, 11-207-733-910, Roche Diagnostic, Basel, Switzerland) Rabbit anti-FG antibody (1:1000, AB153-I, Merck Millipore) Mouse anti-Fos antibody (1:500, ab11959, Abcam)	FITC-Avidin (1:500, A-2001, Vectorlabs) Alexa 647-donkey anti-rabbit (1:500, A31573, Invitrogen) Alexa 594-donkey anti-mouse (1:500, A21203, Invitrogen)
eGFP/Fos/DAPI	Mouse anti-Fos (1:500, ab11959, Abcam)	Alexa 594 donkey anti-mouse (1:500, A21203, Invitrogen)	DAPI (1:500, sc-3598, Santacruz, TX, USA)
Biocytin	594-avidin (1:500, S11227, Invitrogen)		

Supplementary table 3. The company names and serial number of drugs used in experiments

Chemicals	Company names	Serial Number
488-CTB	Invitrogen	A12924
488-Retrobeads	Lumafluor, New York, NY, USA	Cas:78G180
594-Retrobeads	Lumafluor New York, NY, USA	R170
1-fluoro-2,4-dinitrobenzene (DNFB)	Sigma, MO, USA	D1529
Chloroquine (CQ)	Sigma, MO, USA	C6628
Clozapine N-oxide (CNO)	Sigma, MO, USA	C8032
CTB	absin	abs80001
Doxycycline (Dox)	Beyotime, China	ST0398
Fluoro-gold (FG)	Biotium, Hayward, CA, USA	80014
Histamine (His)	Sigma, MO, USA	H7250